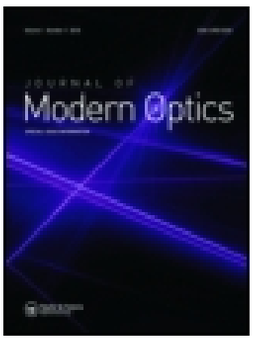

Journal of Modern Optics

ISSN: 0950-0340 (Print) 1362-3044 (Online) Journal homepage: http://www.tandfonline.com/loi/tmop20

Spatial diversity for QAM OFDM RoFSO links with nonzero boresight pointing errors over atmospheric turbulence channels

M. P. Ninos, H. E. Nistazakis, E. Leitgeb & G. S. Tombras

To cite this article: M. P. Ninos, H. E. Nistazakis, E. Leitgeb & G. S. Tombras (2018): Spatial diversity for QAM OFDM RoFSO links with nonzero boresight pointing errors over atmospheric turbulence channels, Journal of Modern Optics, DOI: 10.1080/09500340.2018.1516828

To link to this article: https://doi.org/10.1080/09500340.2018.1516828

Published online: 07 Sep 2018.

JOURNAL OF MODERN OPTICS
https://doi.org/10.1080/09500340.2018.1516828

Taylor & Francis
Taylor & Francis Group

Spatial diversity for QAM OFDM RoFSO links with nonzero boresight pointing errors over atmospheric turbulence channels

M. P. Ninos[a], H. E. Nistazakis[a], E. Leitgeb[b] and G. S. Tombras[a]

[a]Department of Electronics, Computers, Telecommunications and Control, Faculty of Physics, National and Kapodistrian University of Athens, Athens, Greece; [b]Institute of Microwave and Photonic Engineering, Graz University of Technology, Graz, Austria

ABSTRACT

Radio-on-free-space-optical (RoFSO) communication systems have attracted a lot of technological interest in the last few years, due to their high performance characteristics with relatively low installation and operational cost. At the same time a lot of research has been carried out on them. This specific technique facilitates the transmission of radio frequency signals with the aid of optical carriers through the atmosphere; its effectiveness is already known from the Radio over Fibre (RoF) links. However, besides their advantages, the performance of free-space optical (FSO) communication links depends strongly on the atmospheric conditions, due to the fact that the propagation path is the atmosphere. In the present work, we consider the transmission of OFDM radio signals, with QAM modulation format, through an FSO link, using spatial diversity of the receivers. For the estimation of the system performance the atmospheric turbulence effect has been modelled by the gamma-gamma distribution, the accuracy of which spans from weak to strong turbulence conditions. Furthermore, the pointing errors effect is studied with the aid of a new generalized distribution that takes account the nonzero boresight displacement of the optical beam from the optical receiver centre. In addition, different spatial jitters are taken into consideration for the two vertical axes of the receiver. Thus, accurate mathematical expressions are extracted, which lead to the estimation of the average BER and the outage probability of a spatially diverse QAM OFDM RoFSO link. Finally, the theoretical results obtained from the derived expressions are verified through the corresponding numerical simulations which are presented at the numerical results section of the manuscript.

ARTICLE HISTORY
Received 28 March 2018
Accepted 9 August 2018

KEYWORDS
Optical wireless communications; radio on FSO; OFDM; multiple transmitters; receivers spatial diversity; maximum ratio combining; nonzero boresight pointing errors

1. Introduction

The transmission of radio frequency (RF) signals over optical links, simply known as radio over fibre (RoF) technology, has been deployed over the last few years due to the enormous bandwidth of optical media, the increasing demand for higher capacities, the overall low-cost solution offered and the great potential provided for serving the next generation wireless services (*1*,*2*). This technology already has applications including its usage for remote antenna feeding where multiple RF protocols can be transferred from central base stations (CBS) to remote antenna units (RAUs) simultaneously using wavelength division multiplexing (WDM) technique or with subcarrier-multiplexed (SCM) architecture (*2*). In an analogous manner, radio on free-space optical systems (RoFSO) can be deployed effectively, even if the propagation medium is the atmosphere, providing performance features similar to the RoF technology (*3*).

In spite of the fact that RoF is an established technique, the requirement for fibre cable infrastructure has changed attitude towards FSO communications. Thus, FSO systems are also considered for RF signal transmission via line-of-sight links, offering fibre-like bandwidth, license-free and full-duplex connectivity through the atmosphere. This means that RoFSO links can be employed for broadband extension in underserved or urban areas where fibre cable installation is expensive, absent or impossible and also as a fibre backup (*3*–*9*). In (*3*), a WDM RoFSO link is investigated for transmission of different wireless services such as wideband code division multiple access (WCDMA), digital terrestrial television (DTTV) and wireless local area network (WLAN) signals. In Refs (*6*–*8*), point-to-point and multi-hop orthogonal frequency division multiplexing (OFDM) RoFSO links are investigated, which are impaired by atmospheric turbulence and pointing errors with zero boresight. The transmission of long-term evolution (LTE) signals over a dual-polarization RoFSO turbulence channel is studied in (*10*), with the turbulence influence being essential even in weak turbulence

CONTACT Hector E. Nistazakis enistaz@phys.uoa.gr Department of Electronics, Computers, Telecommunications and Control, Faculty of Physics, National and Kapodistrian University of Athens, Athens, 15784, Greece

conditions. In (*11*), the authors study a combined RoF and RoFSO deployment for transmission of LTE signals with dual-polarization.

While it is true that FSO systems have many advantageous features, they actually suffer from the harmful effects of the atmosphere and their performance depends strongly on its characteristics. The atmospheric channel conditions change rapidly because of various phenomena, such as atmospheric turbulence, rain, fog, hail, etc. The atmospheric turbulence results in fast irradiance fluctuations of the optical signal at the receiver, i.e. the so-called scintillation effect. The scintillation effect occurs due to temperature and pressure gradients in the atmospheric layer leading to spatial and temporal irregularities in the refractive index of the atmosphere, (*6*–*18*).

Another essential degradation factor for FSO systems performance is the misalignment-induced fading due to the inevitable motion of the FSO transceivers. These motions can be provoked by strong wind loads, thermal expansions or small earthquakes, (*19*–*28*). Along with the spatial jitter induced by the pointing errors effect, the fixed boresight displacement of the optical beam from the centre of the receiver can cause significant efficiency aggravation (*24*–*28*). In this work, the newly generalized pointing error model is adopted, derived from the Beckmann distribution, which is approximated with a modified Rayleigh distribution. As a result, this pointing error model takes into account the effect of nonzero boresight displacement with different displacements for two vertical axes of each receiver. In addition, different variances (spatial jitters) for the elevation and the horizontal axis of the receivers are considered, (*24*–*26*).

In order to circumvent the aforementioned degradation factors for the performance of the optical wireless links, diversity schemes have been studied and used (*8*,*24*,*29*–*41*). Thus, in (*29*) a subcarrier intensity modulated (SIM) FSO communication system with spatial diversity receivers is studied, while in (*30*) a multi-level polarization shift keying with a maximum ratio combining (MRC) spatial diversity is investigated. Transmit or receive diversity for an on–off keying FSO link is investigated in (*31*,*32*), over K, log normal and gamma gamma turbulence models, assuming uncorrelated or correlated diversity channels. The effect of correlated log normal fading channels for a dual diversity RoFSO link with equal gain combining (EGC) and MRC is presented in (*8*). In (*34*) a performance comparison of different modulation schemes is presented with the exploitation of space diversity either with selection combining (SC) or EGC, while wavelength and time diversity schemes for FSO links are studied in (*37*–*41*).

In OFDM systems the information signal is conveyed by parallel subcarriers which are orthogonal to each other over the OFDM symbol duration (*6*–*9*,*42*–*44*). This technique has already been applied in many digital broadcasting services such as IEEE 802.16e, IEEE 802.11a, g, ac, ad, ax, ay, DTTV, LTE, visible light communications (VLC), etc, and is also considered as a potential candidate for the mobile wireless networks of next generation, i.e. the 5G, (*2*–*6*). Among its advantageous features is the high spectral efficiency, the robustness against frequency selective fading and the inter-symbol interference minimization. Also, simple time-domain equalization is needed. Nonetheless, the main drawback of the OFDM signal is its high peak-to-average power ratios (PAPR), imposing restrictions on its application to intensity modulation schemes such as optical communications (*36*–*38*). A dc bias is required so that clipping of the modulating signal can be avoided. It can lead to nonlinearities though, due to the finite spurious-free dynamic range (SFDR) of the transmitter laser diodes (LD), (*1*,*2*,*6*–*8*,*42*–*44*).

In this work, an OFDM RoFSO communication system with MRC spatial diversity on the receivers is investigated. It is worth pointing out that the specific spatially diverse RoFSO link exploits the usage of multiple laser sources where each one of them is directed towards a specific receiver. In this way, the collected optical radiation for each diversity branch is expected to be augmented significantly. Thus, the performance of the link is assessed in terms of its average bit error rate (BER) and its outage probability (OP), when the signal propagation is corrupted by both atmospheric turbulence and nonzero boresight pointing errors.

The remainder of the manuscript is organized as follows: in section 2 the system setup is presented, while in section 3 the atmospheric turbulence channel and the generalized pointing errors are elaborated. Next, in section 4, closed-form expressions are obtained for the estimation of the average BER of the K-QAM OFDM RoFSO link with diversity on the receivers, while in section 5 the OP expression is extracted. In section 6, the numerical results are presented for various turbulence conditions, spatial jitter influence and spatial diversity configurations. In the last section, the conclusions of this work are summarized.

2. The RoFSO communication system with spatial diversity

The spatial diversity of the receivers is used in wireless communication systems in order to combat fading and improve their performance characteristics. Thus, the OFDM RoFSO link with spatial diversity on the receivers can be realized when a composite transmitter, with M laser sources, sends at the same time moment copies of

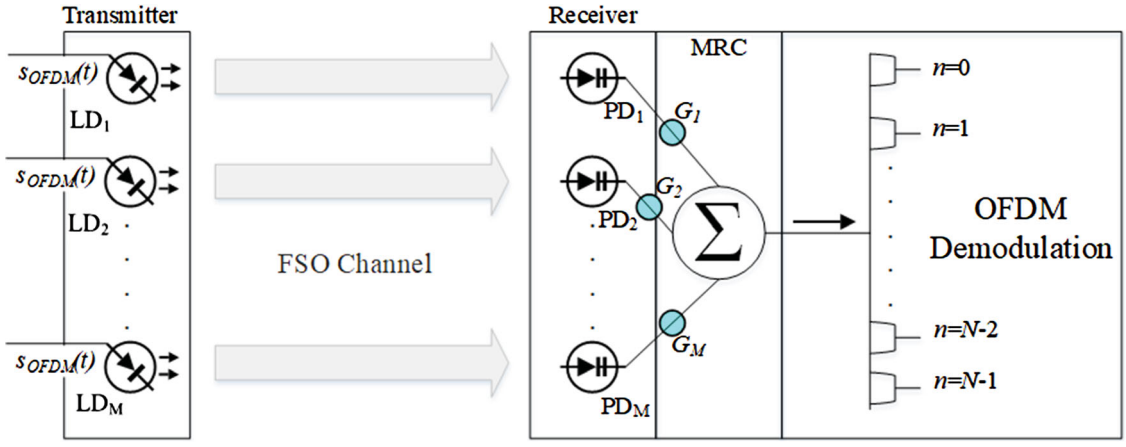

Figure 1. Schematic diagram of the OFDM RoFSO link with multiple laser sources and spatial diversity on the receivers.

the same signal to a set of M receivers, see Figure 1. They are located at distances of a few centimetres apart so as to be uncorrelated (*26–31*). The channel is assumed as memoryless, stationary and ergodic with independent and identically (i.i.d.) distributed intensity random variables for each optical channel. Intensity modulation with direct detection (IM/DD) is employed and the channel state information (CSI) is available both at the transmitter and the MRC receiver (*29–31*).

The OFDM signal, just before the LD and after the up-conversion to the carrier frequency f_c is given as (*3,4,6*):

$$s_{OFDM}(t) = \sum_{n=0}^{N-1} s_n(t) = \sum_{n=0}^{N-1} X_n \exp\left[i2\pi\left(\frac{n}{T_s} + f_c\right)t\right] \quad \text{for} \quad 0 \le t < T_s \tag{1}$$

where N stands for the total number of the subcarriers, T_s stands for the OFDM symbol duration and X_n is the complex data symbol of the n_{th} subcarrier of which the selected modulation format is the QAM scheme, (*1,2,5,6*). Generally, the output of the inverse fast Fourier transform (IFFT) is bipolar, so a dc bias is added prior to the driving of the LD. Since the unipolarity of the OFDM signal, $s_{OFDM}(t)$, is fulfilled, it subsequently modulates the optical intensity of the LDs. The nonlinear response of the LDs can be modelled through nonlinear expressions or series (*1,2*). Thus, the transmitted optical power from each laser source, $P_t(t)$, can be modelled by the expression (*1,5,6*):

$$P_t(t) \approx P_0\left[1 + \sum_{n=0}^{N-1} m_n s_n(t) + a_3\left(\sum_{n=0}^{N-1} m_n s_n(t)\right)^3\right] \tag{2}$$

where P_0 is the average transmitted optical power, α_3 is the third order nonlinear coefficient and m_n represents the optical modulation index (OMI) for each OFDM subcarrier (*1,6,7*).

The transmitted optical signal, during the propagation through the atmospheric medium, is distorted by turbulence-induced fading, path loss, geometrical loss and the misalignment losses. Thus the received optical power at each photo-detector (PD) of the diversity scheme is given as (*3,6,9*):

$$P_{r,m}(t) = P_t(t)L_{tot,m}I_m + n_m(t) \tag{3}$$

where the subscript m denotes the *m-th* receiver with $m = 1, 2, \ldots, M$, P_t is the transmitted optical power from the LD, $L_{tot,m}$ stands for the total losses of the optical signal for each individual optical path, $n_m(t)$ is the additive white Gaussian noise (AWGN), while I_m is the total normalized instantaneous irradiance at each receiver. The latter is given as a product of two random factors $I_{t,m}$ and $I_{p,m}$, i.e. $I_m = I_{t,m}I_{p,m}$, where $I_{t,m}$ stands for the turbulence effect and follows a gamma-gamma distribution, while $I_{p,m}$ represents the nonzero boresight pointing errors effect and is described by the modified Rayleigh distribution (*21–23*).

By substituting (2) into (3), we obtain the following expression for the output current, $i_m(t,I)$, of each individual diversity branch, (*3,6*):

$$i_m(t,I) \approx I_{ph,m}\left[1 + \sum_{n=0}^{N-1} m_n s_n(t) + a_3\left(\sum_{n=0}^{N-1} m_n s_n(t)\right)^3\right] + n_{opt,m}(t) \tag{4}$$

where $I_{ph,m} = \rho_m P_0 L_{tot,m} I_m$ stands for the dc value of the received photocurrent in the m_{th} diversity branch, ρ_m is the responsivity of each PD, while $n_{opt,m}$ represents the optical link noise with zero mean and variance $N_0/2$, with N_0 being, (*3,5–7*):

$$N_{0,m} = \frac{4K_B TF}{R_L} + 2qI_{ph,m} + {I_{ph,m}}^2(RIN) \tag{5}$$

where K_B is the Boltzmann's constant, T stands for the temperature, F is the noise figure of the receiver, R_L the load resistor at the PD, q is the electron charge and RIN is the relative intensity noise process which is a function of the square of the optical power, (*1–3,6,7*).

Another significant mitigation factor is the intermodulation distortion (IMD) resulting from the nonlinear response of the LD. In the case of OFDM, the IMD noise for each subcarrier in a specific diversity branch, $\sigma^2_{n,IMD,m}$, depends on the parameters a_3, m_n, N, and is given as (*1,6,9*):

$$\sigma^2_{n,IMD,m} = 2\xi\left(2n(N-n+1)+N(N-5)+2 - \frac{(-1)^n-(-1)^{2N+n}}{2}\right)^2 \quad (6)$$

where $\xi = 9a_3^2 m_n^6 I^2_{ph,m}/256$.

The signal power at the output of each PD for a given subcarrier frequency ω_n is $C_{n,m}(I_m) = m_n^2 I^2_{ph,m}/2$ and the instantaneous carrier to noise plus distortion ratio ($CNDR_n$) for each OFDM subcarrier at the output of the m_{th} receiver is given as (*6,7*):

$$CNDR_{n,m}(I_m) = \frac{(m_n \rho_m L_{tot,m} P_0 I_m)^2}{2(N_{0,m}/T_s + \sigma^2_{n,IMD,m})} \quad (7)$$

Assuming that the IMD noise is Gaussian distributed (*6*), the total noise at the denominator of (7) can be assumed as Gaussian and thus the $CNDR_{n,m}$ value of (7) can be accurately approximated as (*6,9*):

$$CNDR_{n,m}(I_m) \approx \frac{m_n^2 \rho_m^2 L^2_{tot,m} P_0^2 I_m^2}{2[(N_{0,m}/T_s)_{AV} + (\sigma^2_{n,IMD,m})_{AV}]} \quad (8)$$

where the subscript AV denotes the average value of the corresponding quantities. Moreover, from (8), the expected value of the $CNDR_{n,m}$ can be given as (*6,7*):

$$CNDR_{n,m,EX} \approx \frac{m_n^2 \rho_m^2 L^2_{tot,m} P_0^2 (E[I_m])^2}{2[(N_{0,m}/T_s)_{AV} + (\sigma^2_{n,IMD,m})_{AV}]} \quad (9)$$

with $E[I_m]$ being the expected value of I_m.

Furthermore, in this work, an MRC diversity combiner is assumed on the receivers' side. In the specific diversity technique, the received signals are weighted with a gain factor G_m, which is proportional to the received signal strength in each diversity branch, (*18,45,46*). After the detection process, the received signals are co-phased and summed coherently and we assume that each diversity branch has the same average noise power. Thus, the output of the MRC diversity scheme is given as (*18,45,46*):

$$CNDR_{n,MRC}(I) = \sum_{m=1}^{M} CNDR_{n,m}(I_m) \quad (10)$$

3. Turbulence and generalized pointing errors

In order to describe accurately the intensity fluctuations caused by the scintillation effect, many statistical distribution models have been proposed, examined and used. More specifically, for weak turbulent strength cases the log normal and the gamma statistical models are suitable (*16,47*). Subsequently, the gamma gamma (GG), the I-K and the M(alaga) distributions have been usually adopted for weak up to strong atmospheric turbulence conditions (*16,47–49*). Furthermore, the K and the negative exponential can be used for strong and saturated turbulence conditions, respectively (*16,47*).

In this work, the GG distribution is studied and the corresponding probability density function (PDF), as a function of $I_{t,m}$, is given as (*6,7,48*):

$$f_{I_{t,m}}(I_{t,m}) = \frac{2(a_m b_m)^{\frac{a_m+b_m}{2}}}{\Gamma(a_m)\Gamma(b_m)} I_{t,m}^{\frac{a_m+b_m}{2}-1} K_{a_m-b_m} \times \left(2\sqrt{a_m b_m I_{t,m}}\right) \quad (11)$$

where $\Gamma(.)$ stands for the standard gamma function, $K_v(.)$ represents the modified Bessel function of the second kind and order v, while the parameters a_m and b_m are related to the link parameters values through the expressions, (*50*):

$$a_m = \left[\exp\left(\frac{0.49\delta_m^2}{(1+0.18\mathrm{d}_m^2+0.56\delta_m^{12/5})^{7/6}}\right)-1\right]^{-1}$$
$$b_m = \left[\exp\left(\frac{0.51\delta_m^2(1+0.69\delta_m^2)^{-5/6}}{(1+0.9\mathrm{d}_m^2+0.62\mathrm{d}^2\delta_m^{12/5})^{5/6}}\right)-1\right]^{-1} \quad (12)$$

with $d_m = R_m\sqrt{kL^{-1}_{S,m}}$, $k = 2\pi/\lambda$ is the optical wavenumber and λ is the operational wavelength. The parameter R_m is the aperture radius of each receiver and the $L_{S,m}$ is the distance between the transmitter and the m-th receiver of the FSO link with spatial diversity. The parameter $\delta_m{}^2$ stands for the Rytov variance and is given as $\delta_m^2 = 0.5C_n^2 k^{7/6} L_{S,m}^{11/6}$ (*51*). Furthermore, the parameter C_n^2 represents the refractive index structure parameter and its value depends on the atmospheric turbulence strength. It normally takes values between 10^{-17} $\mathrm{m}^{-2/3}$ and 10^{-13} $\mathrm{m}^{-2/3}$ for weak to strong atmospheric turbulence conditions (*51–53*).

Another significant phenomenon which affects the optical wireless system performance is the pointing errors effect, (*19–28*), (*50*). In order to investigate it, accurately, we examine the following generalized pointing error model, which takes into account the case of nonzero boresight displacement. The usage of this model

becomes even more essential when considering systems with multiple receivers or multiple transmitters, since the loss of the alignment from at least one individual link is almost inevitable. The PDF of this distribution is given as (25,26):

$$f_{I_{p,m}}(I_{p,m}) = \frac{\xi^2_{\text{mod},m}}{A^{\xi^2_{\text{mod},m}}_{\text{mod},m}} I_{p,m}^{\xi^2_{\text{mod},m}-1} \quad \text{with} \quad 0 \le I_{p,m} \le A_{\text{mod},m} \tag{13}$$

with $\xi_{\text{mod},m} = W_{z,eq,m}/2\sigma_{\text{mod},m}$ and the parameter $\sigma_{mod,m}$ is evaluated as (25,26):

$$\sigma_{\text{mod},m} = \left(\frac{3\mu^2_{x,m}\sigma^4_{x,m} + 3\mu^2_{y,m}\sigma^4_{y,m} + \sigma^6_{x,m} + \sigma^6_{y,m}}{2}\right)^{1/6} \tag{14}$$

where $\mu_{x,m}$, $\mu_{y,m}$, $\sigma_{x,m}$, and $\sigma_{y,m}$ are the four parameters of the Beckmann PDF. The parameters ($\sigma_{x,m}$, $\sigma_{y,m}$) correspond to the standard deviations on the horizontal and the elevation axis of each receiver. The parameters ($\mu_{x,m}$, $\mu_{y,m}$) represent the fixed boresight displacements of the optical beam centre from the centre of the m_{th} receiver for the two vertical axes. The term $A_{mod,m}$ is obtained as (25,26):

$$A_{\text{mod},m} = A_{0,m}\exp\left(\frac{1}{\xi^2_{\text{mod},m}} - \frac{1}{2\xi^2_{x,m}} - \frac{1}{2\xi^2_{y,m}} - \frac{\mu^2_{x,m}}{2\sigma^2_{x,m}\xi^2_{x,m}} - \frac{\mu^2_{y,m}}{2\sigma^2_{y,m}\xi^2_{y,m}}\right) \tag{15}$$

where $\xi_{x,m} = W_{z,eq,m}/2\sigma_{x,m}$ and $\xi_{y,m} = W_{z,eq,m}/2\sigma_{y,m}$ with $W_{z,eq,m}$ being the equivalent beam radius at the receiver and is given through the expression $W^2_{z,eq,m} = \sqrt{\pi}erf(\upsilon_m)W^2_{z,m}/2\upsilon_m\exp(-\upsilon^2_m)$. The parameter $A_{0,m}$ is the fraction of the collected power at $r = 0$ and equals to$A_{0,m} = [erf(\upsilon_m)]^2$ with $\upsilon_m = \sqrt{\pi}R_m/\sqrt{2}W_{z,m}$, where *erf(.)* represents the error function and $W_{z,m}$ is the Gaussian beam footprint on each receiver plane, (24–26,53). The beam waist $W_{z,m}$ at each receiver depends on the initial beam waist $W_{0,m}$ at the transmitter, the refractive index structure parameter, the operational wavelength and the length of the optical link (9,19).

The combined PDF of the total normalized instantaneous irradiance I_m, including the GG turbulence and the nonzero boresight pointing errors effects, is obtained as (25):

$$f_{c,I_m}(I_m) = \frac{a_m b_m \xi^2_{\text{mod},m}}{A_{\text{mod},m}\Gamma(a_m)\Gamma(b_m)} G^{3,0}_{1,3}\left(\frac{a_m b_m I_m}{A_{\text{mod},m}}\middle|\begin{matrix}\xi^2_{\text{mod},m}\\ \xi^2_{\text{mod},m}-1,\ a_m-1,\ b_m-1\end{matrix}\right) \tag{16}$$

where $G^{m,n}_{p,q}[\cdot]$ stands for the Meijer G-function, (54).

4. The average BER of the RoFSO system with receivers spatial diversity

In this section, we estimate the performance of the spatially diverse OFDM RoFSO communication system in terms of the average BER as a function of the expected CNDR per subcarrier at the output of the MRC combiner taking into account the atmospheric turbulence along with the nonzero boresight pointing errors effect. Thus, the average BER for each subcarrier, $P_{b,n,MRC,AV}$, of the K-QAM OFDM RoFSO link with the diversity reception scheme, is estimated through the following multiple integral, (31,32):

$$P_{b,n,MRC,AV} = \int_{\vec{I}} f_{c,\vec{I}}(\vec{I}) P_{b,n,QAM,MRC}(\vec{I})d\vec{I} \tag{17}$$

where the vector $\vec{I} = (I_1, I_2, \ldots, I_M)$ includes all the irradiance values for each link of the receivers diversity scheme (37). The conditional BER for each subcarrier, for the K-QAM modulation using diversity with MRC, is given as (1,6,9):

$$P_{b,n,QAM,MRC}(I_m) = \frac{4(1-K^{-1/2})}{\log_2(K)} Q\left(\sqrt{\frac{3}{K-1}\sum_{m=1}^{M} CNDR_{n,m}(I_m)}\right) \tag{18}$$

In order to estimate the integrals of (17) the following approximation for the Q-function is used (55):

$$Q(x) \approx \frac{1}{24}\left[5\exp(-2x^2) + 4\exp\left(-\frac{11x^2}{20}\right) + \exp\left(-\frac{x^2}{2}\right)\right] \tag{19}$$

Next we substitute the approximation (19) into (18) and its outcome into (17). Furthermore, due to the independency of the I_m vectors, the multiple integral of (17) is transformed to the following summation of products of

one-dimensional integrals (31), (56):

$$P_{b,n,AV} \approx \frac{1-K^{-1/2}}{6\log_2(K)}\left[5\prod_{m=1}^{M}\int_0^{\infty} f_{c,I_m}(I_m)\exp\left(-\frac{6CNDR_{n,m}(I_m)}{K-1}\right)\mathrm{d}I_m + 4\prod_{m=1}^{M}\int_0^{\infty} f_{c,I_m}(I_m)\exp\left(-\frac{33CNDR_{n,m}(I_m)}{20(K-1)}\right)\mathrm{d}I_m + \prod_{m=1}^{M}\int_0^{\infty} f_{c,I_m}(I_m)\exp\left(-\frac{3CNDR_{n,m}(I_m)}{2(K-1)}\right)\mathrm{d}I_m\right] \quad (20)$$

Next, substituting for the joint PDF of the GG turbulence with nonzero boresight pointing errors effects, i.e. Eq. (16), into (20), we conclude to:

$$P_{b,n,AV} \approx \frac{1-K^{-1/2}}{6\log_2(K)} \times\left[5\prod_{m=1}^{M}\Xi_m\int_0^{\infty}\Omega_m(I_m)\exp\left(\frac{6CNDR_{n,m}(I_m)}{1-K}\right)\mathrm{d}I_m + 4\prod_{m=1}^{M}\Xi_m\int_0^{\infty}\Omega_m(I_m)\exp\left(\frac{33CNDR_{n,m}(I_m)}{20(1-K)}\right)\mathrm{d}I_m + \prod_{m=1}^{M}\Xi_m\int_0^{\infty}\Omega_m(I_m)\exp\left(\frac{3CNDR_{n,m}(I_m)}{2(1-K)}\right)\mathrm{d}I_m\right] \quad (21)$$

where $\Xi_m = \frac{a_m b_m \xi^2_{\mathrm{mod},m}}{A_{\mathrm{mod},m}\Gamma(a_m)\Gamma(b_m)}$ and $\Omega_m(I_m) = G^{3,0}_{1,3}\left(\frac{a_m b_m I_m}{A_{\mathrm{mod},m}}\middle|\begin{matrix}\xi^2_{\mathrm{mod},m}\\ \xi^2_{\mathrm{mod},m}-1, a_m-1, b_m-1\end{matrix}\right)$. Then, we express the exponential terms of (21) with the proper Meijer-G function (54) and solving the integrals of (21) with the aid of (54), we finally conclude to a closed-form mathematical expression. The obtained mathematical expression leads to the estimation of the average BER of each one of the N subcarriers of the K-QAM OFDM RoFSO link with M-receivers diversity influenced by GG turbulence channels with nonzero boresight pointing errors:

$$P_{b,n,AV} \approx \frac{1-K^{-1/2}}{6\log_2(K)}\left(5\Phi(2,M)+4\Phi\left(\frac{11}{20},M\right)+4\Phi(0.5,M)\right) \quad (22)$$

where $\Phi(x,M) = \prod_{m=1}^{M}\Lambda_1(m)\Psi_1(x,m)$, $\Lambda_1(m) = \frac{2^{a_m+b_m-3}\xi^2_{\mathrm{mod},m}}{\Gamma(a_m)\Gamma(b_m)\pi}$ and

$$\Psi_1(x,m) = G^{1,6}_{6,3}\left(\frac{48x(1+\xi^{-2}_{\mathrm{mod},m})^2 CNDR_{n,m,EX}}{(K-1)(a_m b_m)^2}\middle| \times \begin{matrix}\frac{1-\xi^2_{\mathrm{mod},m}}{2}, \frac{2-\xi^2_{\mathrm{mod},m}}{2}, \frac{1-a_m}{2}, \frac{2-a_m}{2}, \frac{1-b_m}{2}, \frac{2-b_m}{2}\\ 0, -\frac{\xi^2_{\mathrm{mod},m}}{2}, \frac{1-\xi^2_{\mathrm{mod},m}}{2}\end{matrix}\right)$$

while the $CNDR_{n,m,EX}$ is obtained from (9), and the expected value of I_m is estimated as $E[I_m] = \int_0^{\infty} I_m f_{c,I_m}(I_m)dI_m = A_{\mathrm{mod},m}(1+\xi^{-2}_{\mathrm{mod},m})^{-1}$ (24,57).

Next, from (22) and considering large number of subcarriers, (6), the total average BER of the K-QAM OFDM RoFSO link with spatial diversity impaired by nonzero boresight pointing errors and GG distributed turbulence is given as:

$$P_{b,AV} \approx \frac{1-K^{-1/2}}{6N\log_2(K)}\sum_{n=0}^{N-1}\left(5\Phi(2,M)+4\Phi\left(\frac{11}{20},M\right)+\Phi(0.5,M)\right) \quad (23)$$

5. The outage probability of the RoFSO link with spatial diversity

The OP is a significant availability metric for a communication link because it represents the probability of the received $CNDR_{n,m}(I_m)$ to fall below a critical threshold value which corresponds to the receiver sensitivity. Thus, the OP for the n_{th} subcarrier, in a specific m_{th} diversity branch, is given as (3,6,7):

$$P_{out,n,m} = \Pr(CNDR_{n,m}(I_m) < CNDR_{n,m,th}) = \Pr(I_m < I_{m,th}) = \int_0^{I_{m,th}} f_{c,I_m}(I_m)\mathrm{d}I_m \quad (24)$$

where $I_{m,th} = E[I_m]\sqrt{\frac{CNDR_{n,m,th}}{CNDR_{n,m,EX}}}$. Next, replacing (16) into (24) and solving the obtained integral, the following expression is derived for the OP of the n_{th} subcarrier in a specific m_{th} diversity branch affected by nonzero boresight pointing errors over GG distributed turbulence:

$$P_{out,n,m} = \frac{\xi^2_{\mathrm{mod},m}}{\Gamma(a_m)\Gamma(b_m)}G^{3,1}_{2,4}\left(\frac{a_m b_m}{1+\xi^{-2}_{\mathrm{mod},m}}\sqrt{\frac{CNDR_{n,m,th}}{CNDR_{n,m,EX}}}\middle|\begin{matrix}1, \xi^2_{\mathrm{mod},m}+1\\ \xi^2_{\mathrm{mod},m}, a_m, b_m, 0\end{matrix}\right) \quad (25)$$

Under the assumption that the probability of outage is independent for each one of the M links, the total OP for each OFDM subcarrier for the system with receivers diversity is given as the product of the outage probability of each individual RoFSO link, i.e. $P_{out,n} = \prod_{m=1}^{M} P_{out,n,m}$ (40). So, using eq. (25) we conclude to the following expression:

$$P_{out,n} = \prod_{m=1}^{M} \frac{\xi^2_{\text{mod},m}}{\Gamma(a_m)\Gamma(b_m)} G^{3,1}_{2,4}\left(\frac{a_m b_m}{1+\xi^{-2}_{\text{mod},m}} \sqrt{\frac{CNDR_{n,m,th}}{CNDR_{n,m,EX}}} \middle| \begin{matrix} 1,\ \xi^2_{\text{mod},m}+1 \\ \xi^2_{\text{mod},m},\ a_m,\ b_m,\ 0 \end{matrix} \right) \tag{26}$$

In the case we consider a large number of OFDM subcarriers N, the total OP of the OFDM RoFSO link with diversity, impaired by both nonzero boresight pointing errors and GG turbulence, is obtained as:

$$P_{out} = \frac{1}{N} \sum_{n=0}^{N-1} \left[\prod_{m=1}^{M} \frac{\xi^2_{\text{mod},m}}{\Gamma(a_m)\Gamma(b_m)} G^{3,1}_{2,4}\left(\frac{a_m b_m}{1+\xi^{-2}_{\text{mod},m}} \sqrt{\frac{CNDR_{n,m,th}}{CNDR_{n,m,EX}}} \middle| \begin{matrix} 1,\ \xi^2_{\text{mod},m}+1 \\ \xi^2_{\text{mod},m},\ a_m,\ b_m,\ 0 \end{matrix} \right) \right] \tag{27}$$

6. Numerical results

In this section, the average BER and OP numerical results derived from the mathematical expressions (22), (23) and (26), (27) are presented. More specifically, it is assumed that the length of each individual link of the spatial diversity scheme has been set at $L_{S,m} = 3$ km. The aperture radius of all the receivers is the same and equals to 5 cm and the operating wavelength is fixed at $\lambda = 1.55\mu$m. Since the aforementioned parameters are the same for each individual link, the parameters a_m and b_m of the GG distribution can be considered equal to each other, i.e. $a_1 = a_2 = \ldots = a_m$ and $b_1 = b_2 = \ldots = b_m$. The same assumption takes place for the pointing errors parameters. Additionally, the parameter C_n^2 has been assumed to be either 2×10^{-14} m$^{-2/3}$, 4×10^{-14} m$^{-2/3}$ or 8×10^{-14} m$^{-2/3}$ for weak, moderate or strong turbulence conditions, respectively. It should be mentioned here that the above-derived expressions, i.e. (23) and (27), can give results for any realistic parameter value, providing a useful tool for the designing of efficient OFDM FSO links with diversity reception.

Apart from the results obtained through the expressions (23) and (27), the corresponding integrals have been solved numerically, using a Monte Carlo scheme with 2×10^6 samples. Its outcomes appear in the figures of this section and verify the theoretical outcomes from the above derived mathematical expressions.

We study two cases for the influence of the nonzero boresight pointing errors effect at the system performance. In the first case, we assume weak misalignment impact and the values that have been chosen for the normalized spatial jitters are $\sigma_{x,m}/R_m = 0.2$ and $\sigma_{y,m}/R_m = 0.1$ along with zero boresight displacement i.e. $\mu_{x,m}/R_m = 0$ and $\mu_{y,m}/R_m = 0$. In the second case, we assume enhanced misalignment impact, with the following values of $\sigma_{x,m}/R_m = 0.5$, $\sigma_{y,m}/R_m = 0.2$ and nonzero boresight displacement $\mu_{x,m}/R_m = 0.2$, $\mu_{y,m}/R_m = 0.2$. Additionally, the waists of the Gaussian beams at the transmitter are chosen equal to $W_{0,m} = 4$ cm.

As it is evident from the derived numerical results, the OFDM RoFSO communication link with spatial diversity, achieves adequate performance levels by using two or four receive apertures. An average BER at 10^{-6} for the case of 16-QAM, i.e. Figures 2 and 3, and $C_n^2 = 2 \times 10^{-14}$ m$^{-2/3}$ is attained at $CNDR_{n,m,EX} = 30$ dB with $M = 2$ receivers, while with $M = 4$ receivers the same average BER is achieved at values below 25 dB for the $CNDR_{n,m,EX}$. Also, from Figures 2 and 3, it is deduced that the pointing errors impact is circumvented by the usage of the spatial diversity. The worst case scenario is illustrated in Figure 3, when C_n^2 is equal to 8×10^{-14} m$^{-2/3}$ with enhanced spatial jitters and boresight displacement. In this situation, the average BER metric takes the value at 10^{-6} with $CNDR_{n,m,EX} = 35$ dB and $M = 2$ receivers, while the same average BER is achieved below 25 dB when $M = 4$ receive apertures are employed.

Next, in Figures 4 and 5, the average BER results for the 64-QAM case are shown. An average BER at 10^{-6} for $C_n^2 = 2 \times 10^{-14}$ m$^{-2/3}$ is achieved at $CNDR_{n,m,EX} = 35$ dB with $M = 2$ receivers and at 26 dB with $M = 4$ receivers. When the misalignment influence increases, i.e. in Figure 5, the average BER results remain almost invariant. Assuming again the worst case scenario with $C_n^2 = 8 \times 10^{-14}$ m$^{-2/3}$ and strong jitters with boresight errors, the average BER metric takes the value at 10^{-6} when $CNDR_{n,m,EX} = 40$ dB and $M = 2$. In the case when $M = 4$ receivers are employed in the worst case scenario, 10^{-6} average BER is achieved at 29 dB.

The results concerning the average BER when 256-QAM modulation is employed, for each subcarrier, are shown is Figures 6 and 7. As it is evident, 256-QAM format can be effectively used in a range of $CNDR_{n,m,EX}$ 40–45 dB when $M = 2$ receivers are employed, touching values for the average BER at 1×10^{-6}. In addition, for the case of $M = 4$ receivers, the value

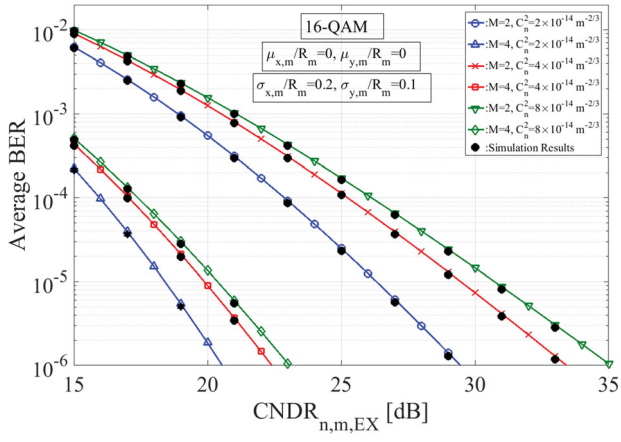

Figure 2. Average BER for the OFDM 16-QAM RoFSO link with receivers diversity as a function of the electrical $CNDR_{n,m,EX}$ per diversity branch for various turbulence conditions, weak spatial jitters and zero boresight displacement.

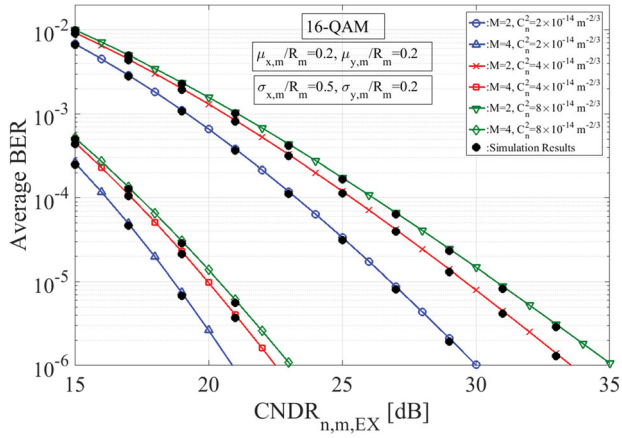

Figure 3. Average BER for the OFDM 16-QAM RoFSO link with receivers diversity as a function of the electrical $CNDR_{n,m,EX}$ per diversity branch for various turbulence conditions, strong spatial jitters and nonzero boresight displacement.

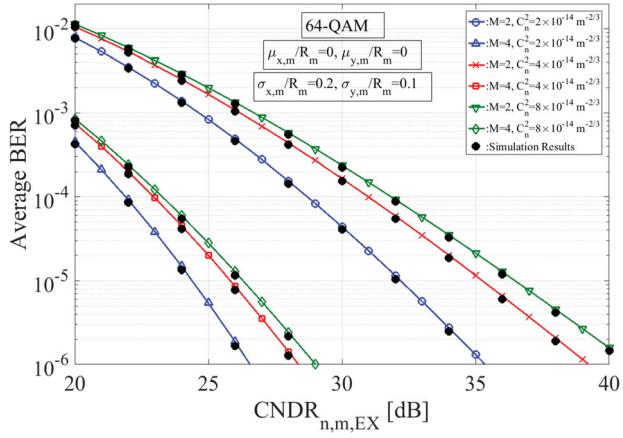

Figure 4. Average BER for the OFDM 64-QAM RoFSO link with receivers diversity as a function of the electrical $CNDR_{n,m,EX}$ per diversity branch for various turbulence conditions, weak spatial jitters and zero boresight displacement.

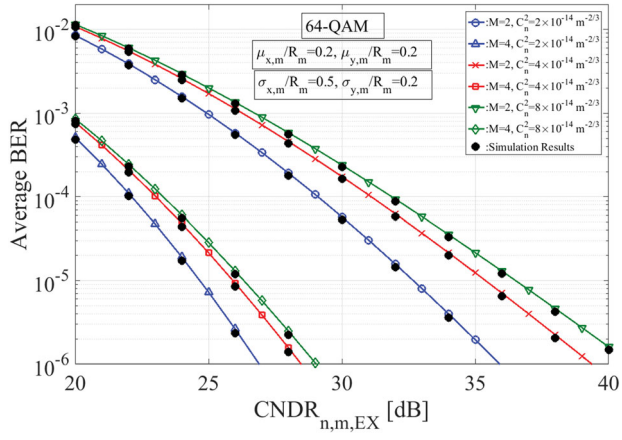

Figure 5. Average BER for the OFDM 64-QAM RoFSO link with receivers diversity as a function of the electrical $CNDR_{n,m,EX}$ per diversity branch for various turbulence conditions, strong spatial jitters and nonzero boresight displacement.

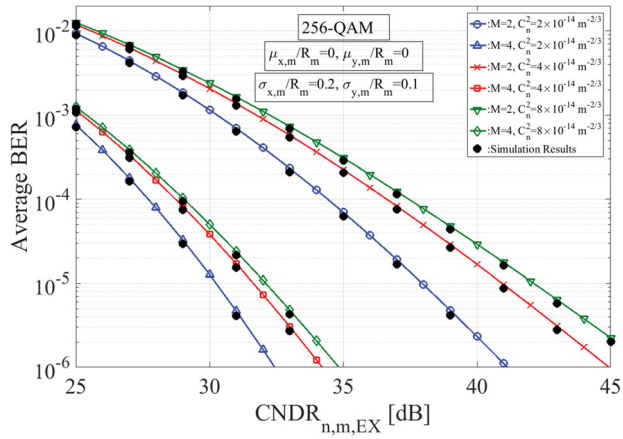

Figure 6. Average BER for the OFDM 256-QAM RoFSO link with receivers diversity as a function of the electrical $CNDR_{n,m,EX}$ per diversity branch for various turbulence conditions, weak spatial jitters and zero boresight displacement.

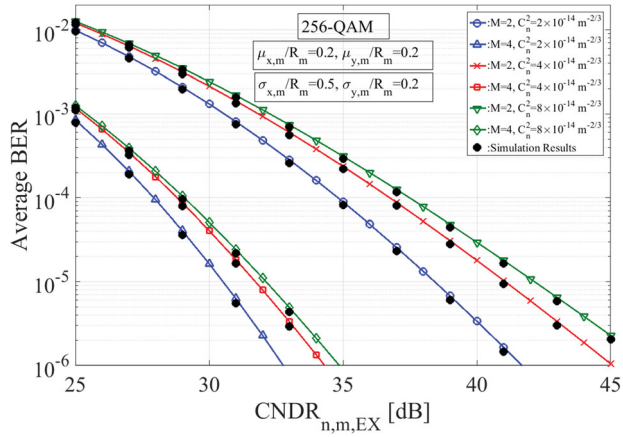

Figure 7. Average BER for the OFDM 256-QAM RoFSO link with receivers diversity as a function of the electrical $CNDR_{n,m,EX}$ per diversity branch for various turbulence conditions, strong spatial jitters and nonzero boresight displacement.

of $CNDR_{n,m,EX}$ ranges from 30 to 35 dB for the achievement of the aforementioned BER target.

Next, in Figures 8 and 9, the outage probability results are shown. In the first case we assume weak spatial jitters, zero boresight displacement with turbulence conditions ranging from moderate to strong. The availability of the RoFSO communication link with diversity increases essentially. Specifically, in Figure 8, assuming the same threshold value for each photo-detector at 10 dB, the OP reaches the value of 10^{-6} with $C_n^2 = 2 \times 10^{-14}$ m$^{-2/3}$ at $CNDR_{n,m,EX} = 31$ dB and $M = 2$ receive apertures. When $M = 4$ receivers are employed, the OP metric reaches the same value at $CNDR_{n,m,EX} = 26$ dB at the previous mentioned turbulence conditions. It is worth mentioning the case of strong turbulence conditions and increased misalignment impact, i.e. Figure 9, where the OP value of 10^{-6} is achieved with $M = 2$ receivers at $CNDR_{n,m,EX} = 38$ dB and the same OP value is attained at $CNDR_{n,m,EX} = 25$ dB with $M = 4$ apertures.

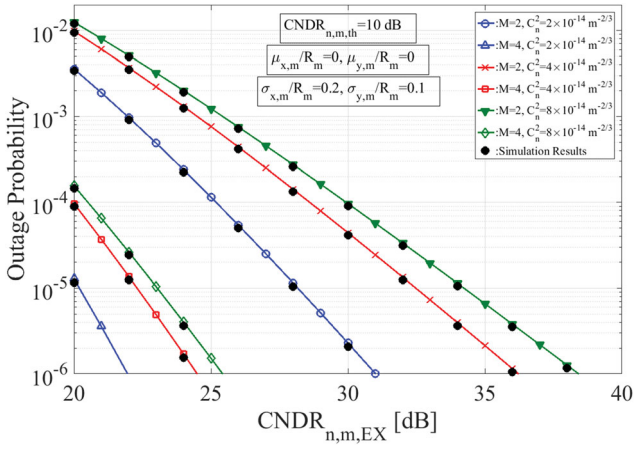

Figure 8. The Outage Probability for the OFDM RoFSO link with receivers diversity for $CNDR_{n,m,th}$ = 10dB as a function of the $CNDR_{n,m,EX}$ per diversity branch for various turbulence conditions, weak spatial jitters and zero boresight displacement.

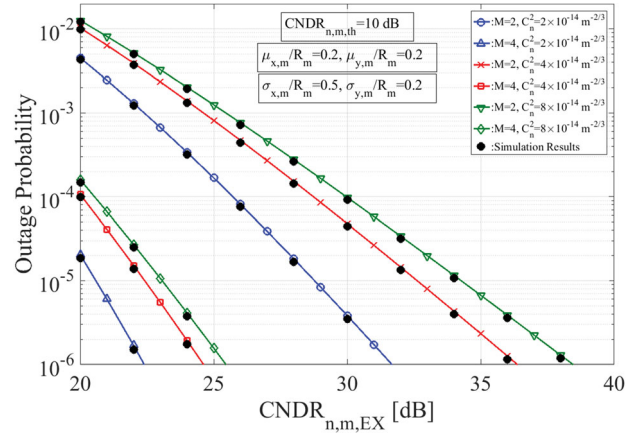

Figure 9. The Outage Probability for the OFDM RoFSO link with receivers diversity for $CNDR_{n,m,th}$ = 10dB as a function of the $CNDR_{n,m,EX}$ per diversity branch for various turbulence conditions, strong spatial jitters and nonzero boresight displacement.

7. Conclusions

In this work, we investigate an OFDM RoFSO communication system with receivers diversity influenced by nonzero boresight pointing errors and GG atmospheric turbulence. The transmitter is composed of multiple laser sources equal to the number of the receive apertures, where each laser transmits towards a specific receiver. The performance of the communication system has been studied by means of the estimation of its average BER and OP. Accurate closed-form mathematical expressions are extracted for the aforementioned metrics, based on realistic phenomena. As it is depicted in the numerical results section, the reliability and the availability of the OFDM RoFSO link with spatial diversity is enhanced essentially. Even in the most adverse atmospheric turbulent conditions with enhanced misalignment losses, the specific FSO link performs within the acceptable standards. Furthermore, the presented numerical results verify the accuracy of the derived mathematical expressions which can be used for FSO system designing.

Disclosure statement

No potential conflict of interest was reported by the authors.

References

(1) Al-Raweshidy, H.; Komaki, S. *Radio Over Fiber Technologies for Mobile Communications Networks*; Artech House: Norwood, MA, 2002.

(2) Fernando, X.N. *Radio Over Fiber for Wireless Communications: From Fundamentals to Advanced Topics*; Wiley: Hoboken, NJ, 2014.

(3) Kazaura, K.; Wakamori, K.; Matsumoto, M.; Higashino, T.; Tsukamoto, K.; Komaki, S. *IEEE Comm. Mag.* **2010,** *48* (2), 130–137.

(4) Fernando, X.N.; Sesay, A.B. *IEEE T. Vehic. Technol.* **2002**, *51* (6), 1576–1586. DOI: 10.1109/TVT.2002.804841.

(5) Yuen, R.; Fernando, X.N. *Wireless Pers. Commun.* **2005,** *33* (1), 1–20. DOI: 10.1007/s11277-005-8314-0.

(6) Bekkali, A.; Naila, C.B.; Kazaura, K.; Wakamori, K.; Matsumoto, M. *IEEE Photonics. J.* **2010,** *2* (3), 510–520.

(7) Nistazakis, H.E.; Stassinakis, A.N.; Sandalidis, H.G.; Tombras, G.S. *IEEE Photonics. J.* 2015, *7*, 1–11. DOI:10.1109/JPHOT.2014.2381670.

(8) Bai, F.; Su, Y.; Sato, T. *J. ICT.* **2014,** *2* (2), 129–150. DOI: 10.13052/jicts2245-800X.224.

(9) Nistazakis, H.E.; Ninos, M.P.; Tsigopoulos, A.D.; Zervos, D.A.; Tombras, G.S. *J. Mod. Optics.* **2016,** *63* (14), 1403–1413.

(10) Bohata, J.; Zvanovec, S.; Korinek, T.; Mansour Abadi, M.; Ghassemlooy, Z. *Appl. Optics.* **2015,** *54* (23), 7082–7087. DOI: 10.1364/AO.54.007082.

(11) Bohata, J.; Zvanovec, S., Pesek, P., et al. *Appl. Optics.* **2016,** *55* (8), 2109–2116. DOI: 10.1364/AO.55.002109.

(12) Prabu, K.; Bose, S.; Kumar, D.S. Analysis of Optical Modulators for Free-Space Optical Communication Systems and Radio Over Fiber Systems. *Proc. Int. Conf. INDICON.* 2012. DOI: 10.1109/INDCON.2012.6420795.

(13) Ghassemlooy, Z; Popoola, W. O. Terrestrial Free-Space Optical Communications. In *Mobile and Wireless Communications: Network Layer and Circuit Level Design*; Ait Fares, S., Adachi, F., Eds.; 2010. (InTech) ISBN: 978-953-307-042-1.

(14) Uysal, M.; Capsoni, C.; Ghassemlooy, Z.; Boucouvalas, A.; Udvary, E. *Optical Wireless Communications: An Emerging Technology*; Springer, **2016**, ISBN 978-3-319-30201-0.

(15) Henniger, H.; Wilfert, O. *Radioengineering.* **2010,** *19* (2), 203–212.

(16) Majumdar, A.K. *Advanced Free Space Optics (FSO): A System Approach*; Springer: New York, 2015, DOI: 10.1007/978-1-4939-0918-6.

(17) Leitgeb, E.; Gebhart, M.; Birnbacher, U.; Muhammad, S.S.; Chlestil, C. Applications of Free Space Optics for Broadband Access. In *Optical Networks and Technologies. IFIP International Federation for Information Processing, Vol 164*; Kitayama, K. I., Masetti-Placci, F., Prati, G., Eds.; Springer, Boston, MA, 2005, DOI: 10.1007/0-387-23178-1_75.

(18) Ghassemlooy, Z.; Popoola, W.O.; Rajbhandari, S. *Optical Wireless Communications: System and Channel Modelling with Matlab*; CRC Press, Taylor & Francis Group: Boca Raton, FL, 2012.

(19) Farid, A.A.; Hranilovic, S. *J. Lightwave. Technol.* **2007,** *25*, 1702–1710.
(20) Gappmair, W.; Hranilovic, S.; Leitgeb, E. *IEEE Comm. Lett.* **2010,** *14* (5), 468–470.
(21) Sandalidis, H.G.; Tsiftsis, T.A.; Karagiannidis, G.K. *J. Lightwave. Technol.* **2009,** *27* (20), 4440–4445.
(22) Garcia-Zambrana, A.; Castillo-Vazquez, B.; Castillo-Vazquez, C. *Opt. Express.* **2012,** *20* (3), 2096–2109.
(23) Djordjevic, G.T.; Petkovic, M.I. *J Mod. Optics.* **2016,** *63* (8), 715–723.
(24) Varotsos, G.K.; Nistazakis, H.E.; Petkovic, M.I.; Djordjevic, G.T.; Tombras, G.S. *Opt. Commun.* **2017,** *403*, 391–400.
(25) Boluda Ruiz, R.; Garcia-Zambrana, A.; Castillo-Vazquez, C.; Castillo-Vazquez, B. *Opt. Express.* **2016,** *24* (20), 22635–22649. DOI: 10.1364/OE.24.022635.
(26) Boluda Ruiz, R.; Garcia-Zambrana, A.; Castillo-Vazquez, C.; Castillo-Vazquez, B. *IEEE Photonics. J.* 2017, *9* (3), 1–14. DOI: 10.1109/JPHOT.2017.2694707.
(27) Yang, F.; Cheng, J.; Tsiftsis, T.A. *IEEE T. Commun.* 2014, *62* (2), 713–725. DOI: 10.1109/TCOMM.2014.010914.130249.
(28) Wang, J.Y.; Wang, J.B.; Chen, M.Y.; Tang, Y.; Zhang, Y. *IEEE Photonics. J.* 2014, *6*, 4. DOI: 10.1109/JPHOT.2014.2332554.
(29) Popoola, W.O.; Ghassemlooy, Z.; Allen, J.I.H.; Leitgeb, E.; Gao, S. *IET Optoelectron.* **2008,** *2* (1), 16–23. DOI: 10.1049/iet-opt:20070030.
(30) Tang, X.; Ghassemlooy, Z.; Rajbhandari, S.; Popoola, W.O.; Lee, C.G. *J Lightwave. Technol.* **2012,** *30* (16), 2689–2695.
(31) Tsiftsis, T.A.; Sandalidis, H.G.; Karagiannidis, G.K.; Uysal, M. *IEEE T. Wirel. Commun.* **2009,** *8* (2), 951–957. DOI: 10.1109/TWC.2009.071318.
(32) Navidpour, S.M.; Uysal, M.; Kavehrad, M. *IEEE T Wirel. Commun.* **2007,** *6* (8), 2813–2819. DOI: 10.1109/TWC.2007.06109.
(33) Ninos, M.P.; Nistazakis, H.E.; Tombras, G.S. *Optik.* **2017,** *138*, 269–279. DOI: 10.1016/j.ijleo.2017.03.009.
(34) Wang, Z.; Zhong, W.D.; Fu, S.; Lin, C. *IEEE Photonics. J.* **2009,** *1* (6), 277–285. DOI: 10.1109/JPHOT.2009.2039015.
(35) Prabu, K.; Kumar, D.S. *Wireless Pers. Commun.* **2015,** *81* (3), 1143–1157. DOI: 10.1007/s11277-014-2176-2.
(36) Djordjevic, G.T.; Petkovic, M.I.; Anastasov, J.A.; Ivanis, P.N.; Marjanovic, Z.M. *IEEE Photonic. Tech. Lett.* **2016,** *28* (12), 1348–1351. DOI: 10.1109/LPT.2016.2543002.
(37) Nistazakis, H.E. *Optik.* **2013,** *124* (13), 1386–1391. DOI: 10.1016/j.ijleo.2012.03.065.
(38) Xu, F.; Khalighi, A.; Caussé, P.; Bourennane, S. *Opt. Express.* **2009,** *17* (2), 872–887.
(39) Purvinskis, R.; Giggenbach, D.; Henniger, H.; Perlot, N.; David, F. Multiple Wavelength Free-Space Laser Communications. *Proc. SPIE.* **2003,** *4975*, 12–19.
(40) Nistazakis, H.E.; Tombras, G.S. *Opt. Laser Technol.* **2012,** *44* (7), 2088–2094. DOI: 10.1016/j.optlastec.2012.03.021.
(41) Balaji, K.A.; Prabu, K. *Opt. Commun.* **2018,** *410*, 643–651. DOI: 10.1016/j.optcom.2017.11.006.
(42) Tsonev, D.; Sinanovic, S.; Haas, H.J. *J. Lightwave Technol.* **2013,** *31* (18), 3064–3076. DOI: 10.1109/JLT.2013.2278675.
(43) Dimitrov, S.; Sinanovic, S.; Haas, H. *IEEE T. Communications.* **2012,** *60* (4), 1072–1081.
(44) Nistazakis, H.E.; Stassinakis, A.N.; Sinanovic, S.; Popoola, W.O.; Tombras, G.S. *IET Optoelectron.* **2015,** *9* (5), 269–274.
(45) Rappaport, T.S. *Wireless Communications: Principles and Practice*, 2nd ed.; Prentice Hall, **2002**. ISBN: 0130422320.
(46) Simon, M.K.; Alouini, M.S. *Digital Communication Over Fading Channels*, 2nd ed.; Wiley: Hoboken, NJ, 2005.
(47) Epple, B. *IEEE/OSA J. Opt. Commun. Netw.* **2010,** *2* (5), 293–304.
(48) Al-Habash, M.A.; Andrews, L.C.; Phillips, R.L. *Opt Eng.* **2001,** *40* (8), 1554–1562.
(49) Andrews, L.C.; Phillips, R.L. *J. Opt. Soc. Am. A.* **1985,** *2* (2), 160–163.
(50) Gappmair, W.; Nistazakis, H.E. *IEEE/OSA J. Lightwave Technol.* **2017,** *35* (9), 1624–1632. DOI: 10.1109/JLT.2017.2685678.
(51) Andrews, L.C.; Philips, R.L. *Laser Beam Propagation Through Random Media*, 2nd ed.; SPIE: Bellingham, WA, 2005. ISBN: 9780819459480.
(52) Leitgeb, E.; Gebhart, M.; Fasser, P.; Bregenzer, J.; Tanczos, J. Impact of Atmospheric Effects in Free-Space Optics Transmission Systems. *Proc. SPIE 4976, Atmos. Propag.* **2003**. DOI: 10.1117/12.483802.
(53) Gappmair, W. *IET Commun.* **2011,** *5* (9), 1262–1267. DOI: 10.1049/iet-com.2010.0172.
(54) Adamchik, V.S.; Marichev, O.I. The Algorithm for Calculating Integrals of Hypergeometric Type Function and its Realization in Reduce System. *Proc. Int. Conf. Symb. Algebr. Comput.* **1990,** 212–224.
(55) Zhang, Q.; Cheng, J.; Karagiannidis, G.K. *IET Commun.* **2014,** *8* (5), 616–625.
(56) Alouini, M.S.; Simon, M.K. *IEEE T. Commun.* **2000,** *48* (3), 401–415. DOI: 10.1109/26.837044.
(57) Al-Quwaiee, H.; Yang, H.C.; Alouini, M.S. *IEEE T. Wirel. Commun.* **2016,** *15* (9), 6502–6512.